An extension of 2D Janbu's generalized procedure of slices for 3D slope stability analysis I

—Basic theory

ZHANG Junfeng, QI Tao & LI Zhengguo

Institute of Mechanics, Chinese Academy of Sciences, Beijing 100080, China
Correspondence should be addressed to Zhang Junfeng (email: zhangjf@imech.ac.cn)
Received July 1, 2004

Abstract Based on 2D Janbu's generalized procedure of slices (GPS), a new three-dimensional slope stability analysis method has been developed, in which all forces acting on the discretized blocks in static equilibrium are taken into account in all three directions. In this method, the potential sliding mass is divided into rigid blocks and each block is analyzed separately by using both geometric relations and static equilibrium formulations. By introducing force boundary conditions, the stability problem is determined statically. The proposed method can be applied to analyze the stability of slopes with various types of potential sliding surfaces, complicated geological boundaries and stratifications, water pressure, and earthquake loading. This method can also be helpful in determining individual factor of safety and local potential sliding direction for each block. As an extension of 2D Janbu's method, the present method has both the advantages and disadvantages of Janbu's generalized procedure of slices.

Keywords: slope stability analysis, three-dimensional analysis, limit equilibrium.

DOI: 10.1360/04zze7

1 Introduction

Most slope stability analyses were performed under 2D limit equilibrium framework in geotechnical engineering. As indicated by Stark and Eid[1], in the existing 2D methods, the calculation of the factor of safety for a slope was carried out under assuming a plane-strain condition, i.e. the failure surface of the slope was assumed infinitely wide. Although 2D slope stability analysis for a slope was relatively conservative, the developed theories and numerical methods were still valuable. Fellenius's method[2], Bishop's method[3], Janbu's generalized procedure[4,5], Morgenstern and Price's method[6], Spencer's method[7,8], and Sarma's method[9,10] seem to be more classical and popular and have been further collected into a number of commercial codes.

However, most practical slope stability problems require further 3D stability analysis.

As a matter of fact, a number of 3D methods have been developed and applied in practical engineering in the past decades. Baligh and Azzouz[11], Londe et al.[12], Hovland[13], Chen and Chameau[14], Leshchinsky et al.[15,16], Hungr et al.[17,18], Zhang[19], Lam and Fredlund[20], Huang and Tsai[21], Chen et al.[22,23] are among the researchers who presented 3D methods and the numerical results.

Most of the existing 3D methods were based on the assumption that the longitudinal sections of the slip surface were circular, or the whole failure surface was approximately regarded as an elliptic revolution[19]. Up to now, only a few methods can be applied to analyze asymmetrical problems with arbitrary slip surfaces existing widely in practical geotechnical engineering. Chen and Chameau[14] derived a method being considered as an extension of Spencer's method; Zhang[19] proposed a simpler method related Spencer's method; Leshchinsky et al.[15,16] presented a generalized method based on variational principle; Lam and Fredlund's method[20] was based on the assumption of the function of inter-block force, and it was more suitable for symmetrical problem; Chen et al.[22,23] calculated the 3D factors of safety of slopes by using the upper bound theorem.

It is well known that the factor of safety F_2 calculated by 2D method is smaller than F_3 obtained by 3D method, because F_2 is calculated for the most critical 2D section. By examining Chen and Chameau's[14] assumptions and results, Hutchinson and Sarma[24] pointed out that the ratio of F_3/F_2 may approach 1.0 but should never fall below 1.0. Duncan[25] reviewed the existing 3D works since the late 1960s by comparison of F_2 and F_3.

Duncan[25] classified the problems in the existing literature into three categories: 1) slopes with curved plane, or containing corners; 2) slopes subjected to loads of limited extent at the top; and 3) slopes in which the potential failure surfaces are constrained by physical boundaries. Huang[21] summarized 3D works into another two categories: 1) research on the so-called "end effect" or " boundary effect" of 3D slopes; and 2) development of a rigorous method for calculation of factors of safety for slopes.

Usually, the factor of safety of a potential failure slope can be regarded as a measurement of the safety degree of the whole slope in macroscopic view. In addition, the stability analysis should also include the following aspects besides the calculation of the whole factor of safety for the slope: 1) to find out local factor of safety for any part of a slope; 2) to determine the sliding directions at any specified positions of a slope; and 3) to give some advices for practical engineering design. As ones know, most 3D stability analyses are based on the limit equilibrium theory and certain discretization techniques. Therefore there are three reasons for us to be able to achieve the objective above-mentioned by means of developing a more rigorous method: 1) since the whole failure mass is discretized into blocks and the static equilibrium equations are built for each block, the individual factor of safety for each block can be given definitely; 2) by combining the geometric characteristics of slip surface, the sliding direction for each block can be determined; and 3) once the above two studies have been completed, the engineering

design should be focused on coping with the most dangerous area with smaller factor of safety than elsewhere of the slope.

Lam and Fredlund[20] noticed the shortcoming of the 3D analysis about the sliding direction in the existing methods, but their method still failed to find out the correct sliding direction for slopes. Based on 2D Bishop's method, Huang[21] presented a significant work which is capable of predicting both local factor of safety and sliding direction. However, Huang's method can only be applied to a slope with circular slip surfaces. For asymmetrical excavation unloading and geological conditions, as the author mentioned, the method may give an overestimated factor of safety.

With all of the force and moment equilibrium equations being satisfied, 2D Janbu's procedure of slices (GPS) belongs to one of the rigorous methods, which may be applied to various kinds of slip surfaces. It has also been adopted by a number of commercial programs available widely. This paper presents a new 3D limit-equilibrium method for slope stability analysis, in which the factors of safety for each part of the failure mass may be different and the local potential sliding direction is determined. As an extension of 2D Janbu's method, the presented 3D method can be applied to analyzing the stability of slopes with various types of potential sliding surfaces, complicated geological boundaries and stratifications, water pressure, seismic loading, as well as other external loadings.

2 Basic principle and 3D limit equilibrium analysis

2.1 Discretization and the forces on a single block

The discretization process is the same as traditional 2D analysis in which the potential failure mass is divided into vertical rigid slices. The only requirement in the proposed method is that the projection of the discretized blocks on horizontal x-y plane should lie on m rows (parallel to the x-direction) and n columns (parallel to the y-direction) in two perpendicular directions. The normal vector of the bottom surface of each block, namely the slip surface, is represented by that of a fitting plane with two dip angles $\alpha_{xz}^{i,j}$ and $\alpha_{yz}^{i,j}$, and the forces acting on a single block are shown in Fig. 1.

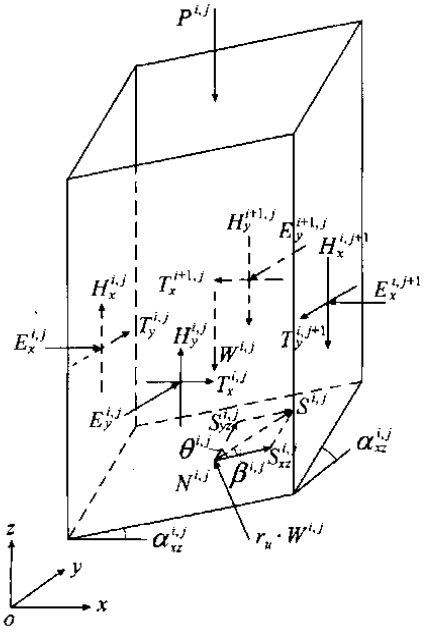

Fig. 1. Schematic diagram of the forces acting on a block.

Nomenclature

m	number of rows to discretize the slope	$\alpha_{yz}^{i,j}$	dip angle of the bottom surface of the block (i,j) with respect to the y direction
n	number of columns to discretize the slope	$\theta^{i,j}$	angle between $S_{xz}^{i,j}$ and $S_{yz}^{i,j}$
i	the ith row	$\beta^{i,j}$	angle between $S_r^{i,j}$ and $S_{yz}^{i,j}$
j	the jth column	$n_x^{i,j}$	x-component of normal vector of the bottom surface of the block (i,j)
(i,j)	serial number of block	$n_y^{i,j}$	y-component of normal vector of the bottom surface of the block (i,j)
$W^{i,j}$	weight of the block (i,j)	$n_z^{i,j}$	z-component of normal vector of the bottom surface of the block (i,j)
$P^{i,j}$	overburden force on the block (i,j)	r_u	pore water pressure coefficient
$N^{i,j}$	normal compressive force on the bottom surface of the block (i,j)	K_{sx}	seismic coefficients corresponding to the x direction
$S_{xz}^{i,j}$	shear force on the bottom surface of the block (i,j) with respect to the direction parallel to the x-z plane	K_{sy}	seismic coefficients corresponding to the y direction
$S_{yz}^{i,j}$	shear force on the bottom surface of the block (i,j) with respect to the direction parallel to the y-z plane	$h_c^{i,j}$	vertical height of the centroid of weight of the block (i,j) to the bottom plane
$S_f^{i,j}$	shear resistance on bottom surface of the block (i,j)	$h_l^{i,j}$	height of the thrust line on the left side of the block (i,j)
$S_r^{i,j}$	real total shear force on bottom surface of the block (i,j)	$h_r^{i,j}$	height of the thrust line on the right side of the block (i,j)
$E_x^{i,j}$	horizontal inter-block thrust force in the x direction	$h_b^{i,j}$	height of the thrust line on the front side of the block (i,j)
$E_y^{i,j}$	horizontal inter-block thrust force in the y direction	$h_u^{i,j}$	height of the thrust line on the back side of the block (i,j)
E_r^i	thrust force acting on the block at the right end of the ith row	Δx	width of block with respect to the x direction
E_l^i	thrust force acting on the block at the left end of the ith row	Δy	width of block with respect to the y direction
E_u^i	thrust force acting on the block at the back end of the jth column	$C^{i,j}$	cohesion of bottom surface of the block (i,j)
E_b^i	thrust force acting on the block at the front end of the jth column	$\varphi^{i,j}$	friction angle of bottom surface of the block (i,j)
$H_x^{i,j}$	vertical inter-block shear force on the inter-block plane perpendicular to the x direction	$A^{i,j}$	area of bottom surface of the block (i,j)
$H_y^{i,j}$	vertical inter-block shear force on the inter-block plane perpendicular to the y direction	$F_x^{i,j}$	factor of safety in the x direction
$T_x^{i,j}$	horizontal inter-block shear force on the inter-block plane parallel to the x-z direction	$F_y^{i,j}$	factor of safety in the y direction
$T_y^{i,j}$	horizontal inter-block shear force on the inter-block plane parallel to the y-z direction	$F^{i,j}$	individual factor of safety of the block (i,j)
$\alpha_{xz}^{i,j}$	dip angle of the bottom surface of the block (i,j) with respect to the x direction	F	the whole factor of safety for a slope

2.2 Basic assumptions

As the deformation is not under consideration in the analysis process, some assumptions should be introduced to render the problem to be solved statically in all the existing limit equilibrium methods. Lam and Fredlund[20] summarized the knowns and unknowns in their method and concluded that the number of assumptions need to be introduced is $8m\times n$ if the slope is discretized into m rows and n columns. In this proposed method, the moment equilibrium equation is built for every block. Thus the number of assumptions must be larger than $8m\times n$. Table 1 shows the relevant knowns and unknowns in this method.

Table 1 Summary of knowns and unknowns for solving 3D factors of safety by the proposed method

Knowns:	
Force equilibrium equations in three directions	$3mn$
Moment equilibrium equations around x and y axes	$2mn$
Mohr-Coulomb failure criteria for slip surfaces	mn
Definitions of $F_x^{i,j}$ and $F_y^{i,j}$	$2mn$
$F_x^{i,j}$ are equal for $i = 1\cdots m, j = 1\cdots n$	$mn-m$
$F_y^{i,j}$ are equal for $i = 1\cdots m, j = 1\cdots n$	$mn-n$
Horizontal thrust forces and vertical shear forces on the left and front boundaries	$2m+2n$
Sums of thrust forces in the x-direction and y-direction, respectively	$m+n$
Subtotal of knowns	$10mn+2m+2n$
Unknowns:	
Forces on slip surfaces	$3mn$
Points of action for forces on slip surfaces	$3mn$
Shear strengths on slip surfaces	mn
Inter-block forces and forces on boundaries	$3m(n+1)+3n(m+1)$
Points of action for inter-block forces and forces on boundaries	$3m(n+1)+3n(m+1)$
$F_x^{i,j}$ and $F_y^{i,j}$	$2mn$
Subtotal for unknowns	$21mn+6m+6n$
Assumptions need to be introduced	$11mn+4m+4n$

Furthermore, in order to solve 3D analysis problems statically, the following assumptions are introduced in this method:

(1) the normal vector of bottom surface for each block is represented by that of a fitting plane; all points of action for forces on bottom surface are at the geometric center (subtotal: $3mn$);

(2) the horizontal inter-block shear forces are neglected, namly $T_x^{i,j} = 0$ and $T_y^{i,j} = 0$ (subtotal: $m(n+1)+n(m+1)$);

(3) the height for the thrust line (in vertical inter-block plane) is a third of the average height of the inter-block quadrangle (subtotal: $3m(n+1)+3n(m+1)$);

(4) forces on boundary are known.

The above assumptions have widely been used in 2D/3D stability analyses and some have been tested by numerical method[20,26]. According to assumption (2), the moment equilibrium equation around z-axis will be automatically satisfied.

2.3 Formulation of the proposed method

To ensure the descretized rigid blocks in equilibrium, the following equations should be satisfied (see Fig. 1):

$$S_{xz}^{i,j}\cdot\cos\alpha_{xz}^{i,j}+(N^{i,j}+r_u\cdot W^{i,j})\cdot n_x^{i,j}-K_{sx}\cdot W^{i,j}+E_x^{i,j}-E_x^{i,j+1}=0\,, \tag{1}$$

$$S_{yz}^{i,j}\cdot\cos\alpha_{yz}^{i,j}+(N^{i,j}+r_u\cdot W^{i,j})\cdot n_y^{i,j}-K_{sy}\cdot W^{i,j}+E_y^{i,j}-E_y^{i+1,j}=0\,, \tag{2}$$

$$\begin{aligned}&S_{xz}^{i,j}\cdot\sin\alpha_{xz}^{i,j}+S_{yz}^{i,j}\cdot\sin\alpha_{yz}^{i,j}+(N^{i,j}+r_u\cdot W^{i,j})\cdot n_z^{i,j}\\&\quad+H_x^{i,j}-H_x^{i,j+1}+H_y^{i,j}-H_y^{i+1,j}-W^{i,j}-P^{i,j}=0,\end{aligned} \tag{3}$$

$$\begin{aligned}&E_y^{i+1,y}\cdot\left(h_u^{i,j}+\frac{1}{2}\Delta y\cdot\tan\alpha_{yz}^{i,j}\right)-E_y^{i,j}\cdot\left(h_b^{i,j}-\frac{1}{2}\Delta y\cdot\tan\alpha_{yz}^{i,j}\right)\\&\quad-H_y^{i+1,j}\cdot\frac{1}{2}\Delta y-H_y^{i,j}\cdot\frac{1}{2}\Delta y+K_{sy}\cdot W^{i,j}\cdot h_c^{i,j}=0,\end{aligned} \tag{4}$$

$$\begin{aligned}&-E_x^{i,j+1}\cdot\left(h_r^{i,j}+\frac{1}{2}\Delta x\cdot\tan\alpha_{xz}^{i,j}\right)+E_x^{i,j}\cdot\left(h_l^{i,j}-\frac{1}{2}\Delta x\cdot\tan\alpha_{xz}^{i,j}\right)\\&\quad+H_x^{i,j+1}\cdot\frac{1}{2}\Delta x+H_x^{i,j}\cdot\frac{1}{2}\Delta x-K_{sx}\cdot W^{i,j}\cdot h_c^{i,j}=0.\end{aligned} \tag{5}$$

According to limit equilibrium, the shear resistance on the bottom surface can be expressed as

$$S_f^{i,j}=C^{i,j}A^{i,j}+N^{i,j}\cdot\tan\varphi^{i,j}\,, \tag{6}$$

where $C^{i,j}$, $\varphi^{i,j}$ and $A^{i,j}$ are cohesion, friction angle, and area of bottom surface of the block (i, j). The factors of safety with respect to the x and y directions are defined like in ref. [21]

$$F_x^{i,j}=\frac{S_f^{i,j}}{S_{xz}^{i,j}}\,, \tag{7}$$

$$F_y^{i,j}=\frac{S_f^{i,j}}{S_{yz}^{i,j}}\,. \tag{8}$$

Obviously the following relation is satisfied

$$F_x^{i,j} \cdot S_{xz}^{i,j} = F_y^{i,j} \cdot S_{yz}^{i,j}. \tag{9}$$

Then the two components of shear force on bottom surface $S_{xz}^{i,j}$ and $S_{yx}^{i,j}$ can be written as

$$S_{xz}^{i,j} = \frac{1}{F_x^{i,j}} \cdot (C^{i,j} A^{i,j} + N^{i,j} \cdot \tan\varphi^{i,j}), \tag{10}$$

$$S_{yz}^{i,j} = \frac{1}{F_y^{i,j}} \cdot (C^{i,j} A^{i,j} + N^{i,j} \cdot \tan\varphi^{i,j}). \tag{11}$$

From eq. (3), the normal force on the bottom surface can be obtained

$$N^{i,j} = \frac{1}{n_z^{i,j}} (W^{i,j} + P^{i,j} + \Delta H_x^{i,j} + \Delta H_y^{i,j} - S_{xz}^{i,j} \cdot \sin\alpha_{xz}^{i,j} - S_{yz}^{i,j} \cdot \sin\alpha_{yz}^{i,j}) - r_u \cdot W^{i,j}, \tag{12}$$

where $\Delta H_x^{i,j} = H_x^{i,j+1} - H_x^{i,j}$ and $\Delta H_y^{i,j} = H_y^{i+1,j} - H_y^{i,j}$, and eq. (12) can be rewritten as

$$N^{i,j} = \frac{(W^{i,j} + P^{i,j} + \Delta H_x^{i,j} + \Delta H_y^{i,j} - n_z^{i,j} \cdot r_u \cdot W^{i,j}) - C^{i,j} A^{i,j} \cdot \left(\dfrac{\sin\alpha_{xz}^{i,j}}{F_x^{i,j}} + \dfrac{\sin\alpha_{yz}^{i,j}}{F_y^{i,j}} \right)}{n_z^{i,j} + \tan\varphi^{i,j} \cdot \left(\dfrac{\sin\alpha_{xz}^{i,j}}{F_x^{i,j}} + \dfrac{\sin\alpha_{yz}^{i,j}}{F_y^{i,j}} \right)}. \tag{13}$$

Substituting eq. (12) into eqs. (10) and (11) and combining eq. (9), $S_{xz}^{i,j}$ and $S_{yx}^{i,j}$ are expressed as

$$S_{xz}^{i,j} = \frac{1}{F_x^{i,j}} \cdot \frac{n_z^{i,j} C^{i,j} A^{i,j} + \tan\varphi^{i,j} \cdot (W^{i,j} + P^{i,j} + \Delta H_x^{i,j} + \Delta H_y^{i,j} - {}_z^{i,j} \cdot r_u \cdot W^{i,j})}{n_z^{i,j} + \tan\varphi^{i,j} \cdot \left(\dfrac{\sin\alpha_{xz}^{i,j}}{F_x^{i,j}} + \dfrac{\sin\alpha_{yz}^{i,j}}{F_y^{i,j}} \right)}, \tag{14}$$

$$S_{yz}^{i,j} = \frac{1}{F_y^{i,j}} \cdot \frac{n_z^{i,j} C^{i,j} A^{i,j} + \tan\varphi^{i,j} \cdot (W^{i,j} + P^{i,j} + \Delta H_x^{i,j} + \Delta H_y^{i,j} - n_z^{i,j} \cdot r_u \cdot W^{i,j})}{n_z^{i,j} + \tan\varphi^{i,j} \cdot \left(\dfrac{\sin\alpha_{xz}^{i,j}}{F_x^{i,j}} + \dfrac{\sin\alpha_{yz}^{i,j}}{F_y^{i,j}} \right)}. \tag{15}$$

Then, the shear resistance on bottom surface is obtained

$$S_f^{i,j} = \frac{n_z^{i,j} C^{i,j} A^{i,j} + \tan\varphi^{i,j} \cdot (W^{i,j} + P^{i,j} + \Delta H_x^{i,j} + \Delta H_y^{i,j} - n_z^{i,j} \cdot r_u \cdot W^{i,j})}{n_z^{i,j} + \tan\varphi^{i,j} \cdot \left(\dfrac{\sin\alpha_{xz}^{i,j}}{F_x^{i,j}} + \dfrac{\sin\alpha_{yz}^{i,j}}{F_y^{i,j}} \right)}. \tag{16}$$

Here, the differences of the thrust forces in the x and y directions are denoted as

$$\Delta E_x^{i,j} = E_x^{i,j+1} - E_x^{i,j}, \tag{17}$$

$$\Delta E_y^{i,j} = E_y^{i+1,j} - E_y^{i,j}. \tag{18}$$

From eqs. (1) and (2), $\Delta E_x^{i,j}$ and $\Delta E_y^{i,j}$ are expressed as

$$\Delta E_x^{i,j} = S_f^{i,j} \cdot \left[\frac{\cos\alpha_{xz}^{i,j}}{F_x^{i,j}} - \frac{n_x^{i,j}}{n_z^{i,j}} \cdot \left(\frac{\sin\alpha_{xz}^{i,j}}{F_x^{i,j}} + \frac{\sin\alpha_{yz}^{i,j}}{F_y^{i,j}} \right) \right]$$

$$+ \frac{n_x^{i,j}}{n_z^{i,j}} \cdot (W^{i,j} + P^{i,j} + \Delta H_x^{i,j} + \Delta H_y^{i,j}) - K_{sx} \cdot W^{i,j}, \tag{19}$$

$$\Delta E_y^{i,j} = S_f^{i,j} \cdot \left[\frac{\cos\alpha_{yz}^{i,j}}{F_y^{i,j}} - \frac{n_y^{i,j}}{n_z^{i,j}} \cdot \left(\frac{\sin\alpha_{xz}^{i,j}}{F_x^{i,j}} + \frac{\sin\alpha_{yz}^{i,j}}{F_y^{i,j}} \right) \right]$$

$$+ \frac{n_y^{i,j}}{n_z^{i,j}} \cdot (W^{i,j} + P^{i,j} + \Delta H_x^{i,j} + \Delta H_y^{i,j}) - K_{sy} \cdot W^{i,j}. \tag{20}$$

To obtain the factors of safety, the boundary conditions must be introduced. However, the selection of suitable boundary condition is related to the understanding on the definition of factor of safety. Considering the effect of 3D boundary, the physical interpretation for the factor of safety can be: the values of the factors of safety for the blocks on the same row in the x direction (i.e. $F_x^{i,j}$ in the ith row) are the same, but may be different from the other row in the x direction. The interpretation is also adopted for the factors of safety in the same column in the y direction, namely, $F_y^{i,j}$ for the blocks in the jth column are the same.

According to the above interpretation and assumption (4) in section 2.2, the forces acting on the end blocks of each row/column should be known, i.e.

$$\sum_j \Delta E_x^{i,j} = E_r^i - E_l^i, \tag{21}$$

where E_r^i and E_l^i are the thrust forces acting on the blocks at the right and left ends of the ith row respectively. Hence the factor of safety with respect to the x direction is determined by substituting eq. (19) into eq. (21):

$$F_x^{i,j} = \frac{\sum_j \left[S_f^{i,j} \cdot \left(\frac{n_x^{i,j}}{n_z^{i,j}} \cdot \sin\alpha_{xz}^{i,j} - \cos\alpha_{xz}^{i,j} \right) \right]}{E_l^i - E_r^i + \sum_j \left[\frac{n_x^{i,j}}{n_z^{i,j}} \cdot \left(W^{i,j} + P^{i,j} + \Delta H_x^{i,j} + \Delta H_y^{i,j} - S_f^{i,j} \cdot \frac{\sin\alpha_{yz}^{i,j}}{F_y^{i,j}} \right) \right] - \sum_j K_{sx} \cdot W^{i,j}}. \tag{22}$$

Similarly, considering boundary conditions in the jth column, one can obtain

$$\sum_j \Delta E_y^{i,j} = E_u^i - E_b^i, \tag{23}$$

in which E_u^i and E_b^j are the thrust forces acting on the blocks at the back and front ends of the jth column.

The factor of safety with respect to the y direction can also be obtained:

$$F_y^{i,j} = \frac{\sum_i \left[S_f^{i,j} \cdot \left(\frac{n_y^{i,j}}{n_z^{i,j}} \cdot \sin\alpha_{yz}^{i,j} - \cos\alpha_{yz}^{i,j} \right) \right]}{E_b^i - E_u^i + \sum_i \left[\frac{n_x^{i,j}}{n_z^{i,j}} \cdot \left(W^{i,j} + P^{i,j} + \Delta H_x^{i,j} + \Delta H_y^{i,j} - S_f^{i,j} \cdot \frac{\sin\alpha_{xz}^{i,j}}{F_x^{i,j}} \right) \right] - \sum_i K_{sy} \cdot W^{i,j}}. \tag{24}$$

The thrust forces $E_x^{i,j}$ and $E_y^{i,j}$ can be calculated in-order according to eqs. (19) and (20):

$$E_x^{i,j+1} = E_x^{i,j} + S_f^{i,j} \cdot \left[\frac{\cos\alpha_{xz}^{i,j}}{F_x^{i,j}} - \frac{n_x^{i,j}}{n_z^{i,j}} \cdot \left(\frac{\sin\alpha_{xz}^{i,j}}{F_x^{i,j}} + \frac{\sin\alpha_{yz}^{i,j}}{F_y^{i,j}} \right) \right]$$

$$+ \frac{n_x^{i,j}}{n_z^{i,j}} \cdot (W^{i,j} + P^{i,j} + \Delta H_x^{i,j} + \Delta H_y^{i,j}) - K_{sx} \cdot W^{i,j} \tag{25}$$

$$E_y^{i,j+1} = E_y^{i,j} + S_f^{i,j} \cdot \left[\frac{\cos\alpha_{xz}^{i,j}}{F_y^{i,j}} - \frac{n_y^{i,j}}{n_z^{i,j}} \cdot \left(\frac{\sin\alpha_{xz}^{i,j}}{F_x^{i,j}} + \frac{\sin\alpha_{yz}^{i,j}}{F_y^{i,j}} \right) \right]$$

$$+ \frac{n_y^{i,j}}{n_z^{i,j}} \cdot (W^{i,j} + P^{i,j} + \Delta H_x^{i,j} + \Delta H_y^{i,j}) - K_{sy} \cdot W^{i,j}. \tag{26}$$

Eqs. (4), (5), (17) and (18) result in the vertical shear forces acting on the lateral sides neglecting the small quantities with high order:

$$H_x^{i,j} = [E_x^{i,j} \cdot (h_r^{i,j} - h_l^{i,j}) + \Delta E_x^{i,j} \cdot h_l^{i,j} + K_{sx} \cdot W^{i,j} \cdot h_c^{i,j}] \cdot \frac{1}{\Delta x}, \tag{27}$$

$$H_y^{i,j} = [E_y^{i,j} \cdot (h_u^{i,j} - h_b^{i,j}) + \Delta E_y^{i,j} \cdot h_b^{i,j} + K_{sy} \cdot W^{i,j} \cdot h_c^{i,j}] \cdot \frac{1}{\Delta y}. \tag{28}$$

The factors of safety for each block with respect to the x and y directions have been determined by now, and the acting forces can also be calculated accordingly. To give the real factor of safety and the sliding direction of each block (i.e. the direction of the real mobilized shear force $S_r^{i,j}$), one can combine the two components of the shear force on

the bottom surface to get the real mobilized shear force $S_r^{i,j}$

$$S_r^{i,j} = \sqrt{(S_{xz}^{i,j})^2 + (S_{yz}^{i,j})^2 + 2 \cdot S_{xz}^{i,j} \cdot S_{yz}^{i,j} \cdot \sin\alpha_{xz}^{i,j} \cdot \sin\alpha_{yz}^{i,j}} \,. \tag{29}$$

Then the real factor of safety of the block (i, j) is expressed by its definition

$$F^{i,j} = \frac{S_f^{i,j}}{S_r^{i,j}} \,. \tag{30}$$

The relationships between $F_x^{i,j}$, $F_y^{i,j}$ and $F^{i,j}$ can be obtained from the force triangle formed by $S_{xz}^{i,j}$, $S_{yz}^{i,j}$ and $S_r^{i,j}$ on the bottom surface of the block (i, j) according to the law of sine[21]. The sliding direction of the block is determined by the angle $\beta^{i,j}$ between $S_r^{i,j}$ and $S_{xz}^{i,j}$, and $\beta^{i,j}$ satisfies the following expression:

$$\sin\beta^{i,j} = \frac{F^{i,j}}{F_y^{i,j}} \cdot \sin\theta^{i,j} \,, \tag{31}$$

where $\theta^{i,j}$ is the angle between $S_{xz}^{i,j}$ and $S_{yz}^{i,j}$ and can be determined by the geometric characteristic of the bottom surface of the block.

In fact, when the factor of safety of each block is determined, the stability problem of the slope should be focused on determination of the most dangerous position and the sliding direction. However, the factor of safety for the failure mass as a whole can still be given as conventional 2D and 3D analyses by the following definition:

$$F = \frac{\sum\limits_i \sum\limits_j S_f^{i,j}}{\sum\limits_i \sum\limits_j S_r^{i,j}} \,. \tag{32}$$

3 Validity of the proposed method

Two examples are used to verify the validity of this method. The first example is from Zhang[19] which is a symmetrical problem with the slip surface being regarded as an elliptic revolution (Figs. 2—4). The second example is an asymmetrical one, the slip surface of which is featured with part of an ellipsoidal surface, but the lengths of the three axes are different (Fig. 5, Fig. 6).

3.1 Example 1

Figs. 2—4 show the geometric characteristics of the failure mass (see refs. [19, 20, 22]). The calculated factors of safety using the present method are summarized in Table 2 for the slope under six conditions. The factor of safety and sliding direction of each block will be presented in Part II of this paper in detail. Results obtained by Zhang[19] are

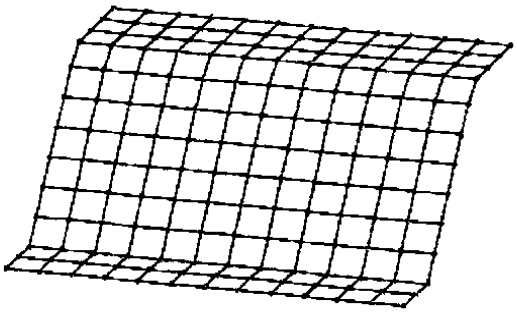

Fig. 2. Top surface of the slope in example 1.

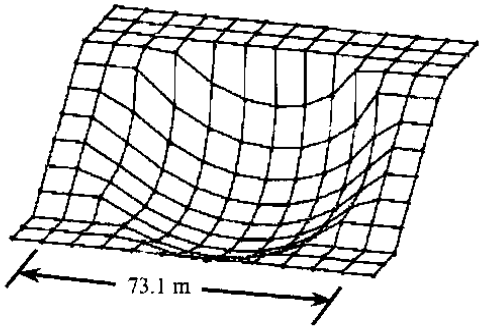

Fig. 3. Concave slip surface in example 1.

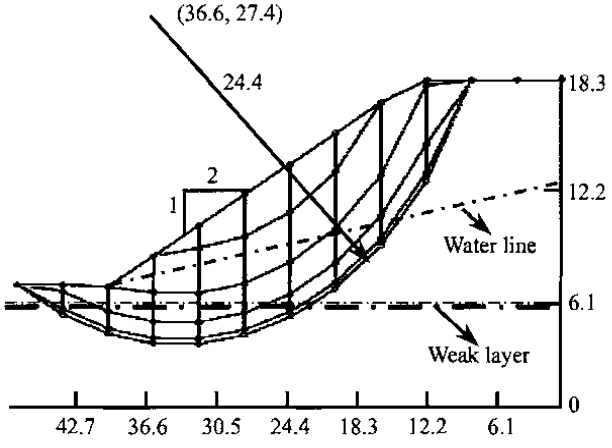

Fig. 4. Longitudinal sections and geometric size of the slope.

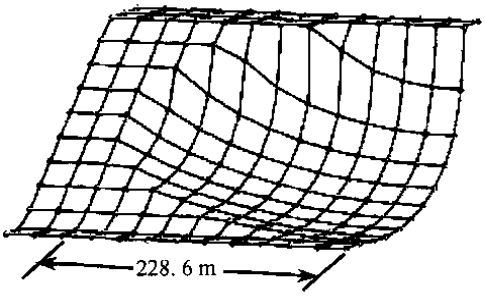

Fig. 5. Ellipsoidal slip surface in example 2.

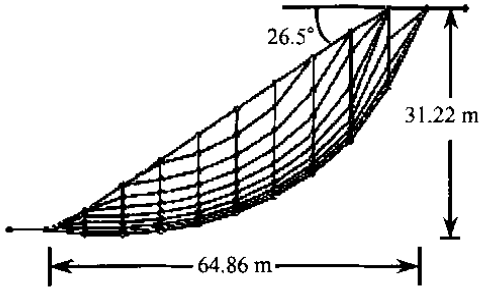

Fig. 6. Longitudinal sections of the slope.

Table 2 Comparison of factors of safety for a slope under six conditions

Example 1	Simple slope			With a thin weak layer		
	Regardless of water pressure	Water pressure $r_u = 0.25$	With a piezometric line	Regardless of water pressure	Water pressure $r_u = 0.25$	With a piezometric line
The proposed method	2.126	1.858	1.935	1.611	1.394	1.513
Zhang's method	2.122	1.790	1.831	1.548	1.278	1.441

also given in Table 2. The factor of safety of the simple slope calculated by the upper bound theorem in ref. [22] is 2.262.

3.2 Example 2

Similar to example 1, the top surface of the slope used in example 2 is still a plane, but the dip angle is 26.5°. The slip surface (half an ellipsoid) and the longitudinal sections of the slope are shown in Figs. 5 and 6. The ellipsoidal slip surface can be expressed as

$$\frac{x^2}{a^2}+\frac{(y-y_0)^2}{b^2}+\frac{(z-z_0)^2}{c^2}=1, \tag{33}$$

in which y_0 = 9.6 m and z_0 = 31.22 m, a, b and c the half-length of the ellipsoidal axes in x, y and z directions respectively (here, a = 300 m, b = 55.26 m and c = 31.22 m).

The factor of safety calculated by this proposed method is 2.228 for the simple slope. Provided with the ratio of water pressure r_u = 0.25, the proposed method produces the factor of safety 1.694. The calculated results of the factors of safety and sliding directions for a similar example with geometrical asymmetry are presented in Part II of this paper also.

4 Concluding remarks

In conventional stability analysis by using limit equilibrium method, the factor of safety for a slope is for the whole failure mass, assuming that each slice/block has the same factor of safety value. In the present method, each block is subjected to the action of forces from both horizontal and longitudinal directions. Hence, it is certain that the block has two factors of safety with respect to two directions, and the real factor of safety of the block is obtained by combining the two component factors of safety. The sliding direction of each block can also be determined by using the geometric characteristics. Thus the blocks of a slope may have different values of factors of safety and sliding directions. This is reasonable and conceivable.

Different interpretations for the factor of safety may lead to different results for the factor of safety. In the present method, one can consider the blocks in the same row as a 2D problem with force condition being provided in the third dimension. Such a consideration can sufficiently reflect the boundary effect and the geometric feature of slip surface.

Acknowledgements The authors wish to thank all their colleagues in the Institute of Mechanics, CAS, for their valuable discussion on various parts of the work described in the paper. This work was supported by the National Natural Science Foundation of China (Grant No. 10372104), the Special Funds for the Major State Basic Research Project (Grant No. 2002CB412706), the Knowledge Innovation Project of the Chinese Academy of Sciences (Grant No. KJCX2-SW-L1-2), the Special Research Project for Landslide and Bank-collapse in The Three Gorges Reservoir Areas (Grant No. 4-5).

References

1. Stark, T. D., Eid, H. T., Performance of three-dimensional slope stability methods in practice, J. of Geotech-

nical and Geoenvironmental Engineering, 1998, 124(11): 1049—1060.
2. Fellenius, W., Calculation of the stability of earth dams, Proceedings of the Second Congress of Large Dams, 1936, 4: 445—463.
3. Bishop, A. W., The use of the slip circle in the stability analysis of slopes, Geotechnique, 1955, 5(1): 7—17.
4. Janbu, N., Earth pressure and bearing capacity by generalized procedure of slices, Proceedings of the 4th Int. Conf. of Soil Mechanics, London, Butterworths Scientific Publications, 1957, 2: 207—212.
5. Janbu, N., Slope stability computations, in Embankment-Dam Engineering, New York: John Wiley and Sons, 1973, 47—86.
6. Morgenstern, N. R., Price, V. E., The analysis of the stability of general slip surfaces, Geotechnique, 1965, 15: 79—93.
7. Spencer, E., A method of analysis of the stability of embankments assuming parallel inter-slice forces, Geotechnique, 1967: 17(1): 11—26.
8. Spencer, E., Thrust line criterion in embankment stability, Geotechnique, 1973, 23(1): 85—100.
9. Sarma, S. K., Stability analysis of embankment and slopes, Geotechnique, 1973; 23(3): 423—433.
10. Sarma, S. K., Stability analysis of embankment and slopes, J. of the Geotechnical Engineering Division, Proceeding of the American Society of Civil Engineers, 1979, 105(GT12): 1511—1522.
11. Baligh, M. M., Azzouz, A. S., End effects on stability of cohesive slopes, J. of Geotechnical Engineering Division, Proceeding of the American Society of Civil Engineers, 1975, 101(GT11): 1105—1117.
12. Londe, P., Vigier, G., Vormeringer, R., Stability of rock slopes, a three-dimensional study, Soil Mechanics and Foundations Division, Proceeding of the American Society of Civil Engineers, 1969, 95(SM1): 235—262.
13. Hovland, H. J., Three-dimensional slope stability analysis method, J. of Geotechnical Engineering Division, Proceeding of the American Society of Civil Engineers, 1976, 103(GT9): 971—986.
14. Chen, R. H., Chameau, J. L., Three-dimensional limit equilibrium analysis of slope, Geotechnique, 1982, 32(1): 31—40.
15. Leshchinsky, D., Baker, R., Silver, M. L., Three-dimensional analysis of slope stability, Int. J. for Numerical and Analytical Methods in Geomechanics, 1985, 9: 199—223.
16. Leshchinsky, D., Huang, C. C., Generalized three-dimensional slope-stability analysis, J. Geotechnical Engineering, 1992, 118(11): 1748—1764.
17. Hungr, O., An extension of Bishop's simplified method of slope stability analysis to three dimensions, Geotechnique, 1987, 37: 113—117.
18. Hungr, O., Salgado, F. M., Byrue, P. M., Evaluation of a three-dimensional method of slope stability analysis, Can. Geotech. J., 1988, 26: 679—686.
19. Zhang, X., Three-dimensional stability analysis of concave slopes in plane view, J. of Geotechnical Engineering, 1988, 114(6): 658—671.
20. Lam, L., Fredlund, D. G., A general limit equilibrium model for three-dimensional slope analysis, Canadian Geotechnical Journal, 1993, 30: 905—919.
21. Huang, C. C., Tsai, C. C., New method for 3D and asymmetrical slope stability analysis, J. of Geotechnical and Geoenvironmental Engineering, 2000, 126(10): 917—927.
22. Chen, Z., Wang, X., Haberfield, C. et al., A three-dimensional slope stability analysis method using the upper bound theorem, Part I: theory and methods, Int. J. Rock Mech. Min. Sci., 2001, 38: 369—378.
23. Chen, Z., Wang, J., Wang, Y. et al., A three-dimensional slope stability analysis method using the upper bound theorem, Part II: numerical approaches, applications and extensions, Int. J. Rock Mech. Min. Sci., 2001, 38: 379—397.
24. Hutchinson, J. N., Sarma, S. K., Discussion on "Three-dimensional limit equilibrium analysis of slopes", Geotechnique, 1985, 35(2): 215—216.
25. Duncan, J. M., State of the art: limit equilibrium and finite-element analysis of slopes, J. Geotechnical Engineering, 1996, 122(7): 577—596.
26. Fan, K., Fredlund, D. G., Wilson, G. W., An interslice force function for limit equilibrium slope stability analysis, Canadian Geotechnical Journal, 1986, 23: 287—296.